Proceedings of the 30th International Cosmic Ray Conference
Rogelio Caballero, Juan Carlos D'Olivo, Gustavo Medina-Tanco,
Lukas Nellen, Federico A. Sánchez, José F. Valdés-Galicia (eds.)
Universidad Nacional Autónoma de México,
Mexico City, Mexico, 2008

Vol. 2 (OG part 1), pages 699–702

30TH INTERNATIONAL COSMIC RAY CONFERENCE

ICRC'07 Mérida, México

Observations of microquasars with the MAGIC telescope

JAVIER RICO[1,*] MICHAEL RISSI[2], POL BORDAS[3], VALENTI BOSCH-RAMON[3], JUAN CORTINA[1], JOSEP M. PAREDES[3], MARC RIBÓ[3], DIEGO F. TORRES[4] AND ROBERTA ZANIN[1] FOR THE MAGIC COLLABORATION

[1]*Institut de Fisica d'Altes Energies, Barcelona, Spain*
[2]*Institute for Particle Physics, ETH Zurich, Switzerland*
[3]*Departament d'Astronomia i Meteorologia, Universitat de Barcelona, Barcelona, Spain*
[4]*ICREA & Institut de Ciencies de l'Espai (IEEC-CSIC), Barcelona, Spain*
[*]*Presenter (jrico@ifae.es)*

Abstract: We report on the results from the observations in very high energy band (VHE, $E_\gamma \geq 100$ GeV) of the black hole X-ray binary (BHXB) Cygnus X-1. The observations were performed with the MAGIC telescope, for a total of 40 hours during 26 nights, spanning the period between June and November 2006. We report on the results of the searches for steady and variable γ-ray signals, including the first experimental evidence for an intense VHE flare, of duration between 1.5 and 24 hours.

Cygnus X-1 is the best established candidate for a stellar mass black-hole (BH) and one of the brightest X-ray sources in the sky [1]. Located at a distance of 2.2 ± 0.2 kpc, it is composed of a 21 ± 8 M$_\odot$ BH orbiting an O9.7 Iab companion of 40 ± 10 M$_\odot$ [2] in a circular orbit of 5.6 days and inclination between 25° and 65° [3]. The X-ray source is likely powered by accretion and displays the canonical high/soft and low/hard X-ray spectral states. The thermal soft component is produced by the accretion disk close to the BH, whereas hard X-rays are thought to be produced by inverse Compton scattering of soft photons by thermal electrons in a corona or at the base of a relativistic jet. Observations in the soft γ-ray range with COMPTEL [4] and *INTEGRAL* [5] strongly suggest the presence of a higher energy, non-thermal component.

Images with the VLBA have shown the presence of a highly collimated relativistic jet [6]. Some authors have suggested that Cygnus X-1 could be a "microblazar", where the jet axis is roughly aligned with the line of sight [7]. The interaction of the jet with the interstellar medium appears to be responsible for a large-scale (~ 5 pc diameter), ring-like, radio emitting structure [8].

Three other binary systems have been detected so far in the VHE domain: PSR B1259−63 [9], LS I +61 303 [10] and LS 5039 [11]. In PSR B1259−63 the TeV emission is thought to be produced by the interaction of the relativistic wind from a young pulsar with the outflow of the companion star. Recent results suggest that LS I +61 303 also contains a non-accreting neutron star [12], while the situation is not yet clear for LS 5039 [13, 14]. To date, however, there is no experimental evidence of VHE emission from any Galactic BHXB system.

Cygnus X-1 was observed with MAGIC between June and November 2006 [15]. The data set comprises 40.0 good observation hours from 26 different nights (see Table 1 for details). A search for *steady* γ-ray signals was performed for the entire recorded data sample, yielding no significant excess. This allows us to establish the first upper limits to the VHE γ-ray steady flux of Cygnus X-1 in the range between 150 GeV and 3 TeV (see Figure 1), of the order of $\sim 1-5\%$ of the Crab nebula flux. Given the timescale of the variability of Cygnus X-1 in other energy bands, γ-ray signals were also searched for on a daily basis. The results are shown in Table 1. We obtain results compatible with background fluctua-

MJD [days]	T [min]	Nexcess [evts]	S [σ]	Post [σ]
53942.051	61.1	3.6± 4.8	0.8	< 0.1
53964.887	105.6	4.8± 6.9	0.7	< 0.1
53965.895	195.3	−13.2± 10.1	−1.3	< 0.1
53966.934	124.8	9.4± 9.5	1.0	< 0.1
53967.992	48.5	−9.0± 4.7	−1.7	< 0.1
53968.883	237.5	−4.4± 11.6	−0.4	< 0.1
53994.953	53.6	−4.0± 4.9	−0.8	< 0.1
53995.961	58.1	−2.8± 4.6	−0.6	< 0.1
53996.855	176.2	1.6± 9.1	0.2	< 0.1
53997.883	132.7	5.2± 7.6	0.7	< 0.1
54000.852	165.2	11.4± 9.7	1.2	< 0.1
54002.875	154.4	36.8± 10.4	4.0	3.2
54003.859	166.9	−7.0± 9.1	−0.8	< 0.1
54004.891	123.3	−6.0± 7.9	−0.7	< 0.1
54005.914	87.9	−2.2± 6.3	−0.3	< 0.1
54006.938	28.0	5.4± 4.1	1.4	< 0.1
54020.891	65.5	−8.6± 5.9	−1.4	< 0.1
54021.887	68.6	−6.2± 5.7	−1.0	< 0.1
54022.887	58.1	1.6± 5.9	0.3	< 0.1
54028.863	68.6	3.4± 5.9	0.6	< 0.1
54029.895	33.5	3.4± 5.1	0.7	< 0.1
54030.863	19.6	−1.8± 3.0	−0.6	< 0.1
54048.824	47.2	1.6± 5.7	0.3	< 0.1
54049.824	47.9	−6.0± 5.4	−1.1	< 0.1
54056.820	27.1	−5.2± 3.8	−1.3	< 0.1
54057.820	21.5	1.2± 2.6	0.5	< 0.1

Table 1: From left to right: Modified Julian Date of the beginning of the observation, total effective observation time (EOT), number of excess events, statistical significance of the excess, equivalent (*post-trial*) significance for 26 independent samples. A cut SIZE>200 photo-electrons ($E_\gamma > 150$ GeV) has been applied.

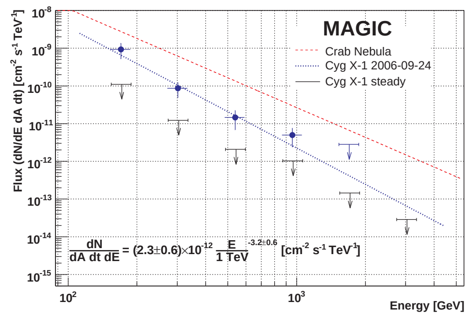

Figure 1: Differential energy spectrum from Cygnus X-1 corresponding to 78.9 minutes EOT between MJD 54002.928 and 54002.987 (2006-09-24). Also shown are the Crab nebula spectrum and the best fit of a power-law to the data and the 95% CL upper limits to the steady γ-ray flux.

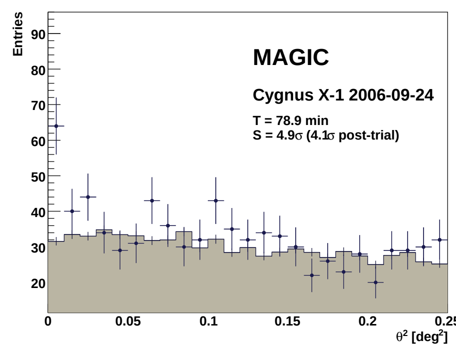

Figure 2: Distribution of θ^2 values for the signal (dots) and background (histogram) events for an energy threshold of 150 GeV.

tions at 99% CL for all searched samples except for MJD=54002.875 (2006-09-24). We derive upper limits to the integral flux above 150 GeV between 2 and 25% of the Crab nebula flux (depending basically on the observation time) for all samples compatible with background fluctuations. The data from 2006-09-24 were further subdivided into two halves to search for rapidly varying signals, obtaining 0.5σ and 4.9σ results for the first (75.5 minutes EOT starting at MJD 54002.875) and second (78.9 minutes EOT starting at MJD 54002.928) samples, respectively. The post-trial probability is conservatively estimated by assuming 52 trials (2 per observation night) and corresponds to a significance of 4.1σ. The sample corresponding to MJD 54002.928 was further subdivided into halves, obtaining 3.2σ and 3.5σ excesses in each. At this point we stopped the data splitting process.

The distribution of θ^2 for signal and background events corresponding to the 78.9 minutes EOT sample starting at MJD 54002.928 is shown in Figure 2. The excess is consistent with a point source located at the position of Cygnus X-1. The map of excess events around the source is shown in Figure 3. A Gaussian fit yields the location: $\alpha = 19^{\rm h}58^{\rm m}17^{\rm s}$, $\delta = 35°12'8''$ with statistical and systematic uncertainties of $1.5'$ and $2'$, respectively, compatible within errors with the position of Cygnus X-1 and excluding the radio nebula at a distance of $\sim 8'$. The energy spectrum is shown in Figure 1. It is well fitted ($\chi^2/n.d.f = 0.5$) by the following power law: $dN/(dA\ dt\ dE) = (2.3 \pm$

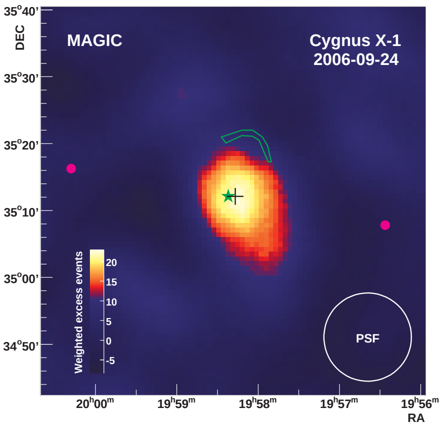

Figure 3: Gaussian-smoothed ($\sigma = 4'$) map of γ-ray excess events (background subtracted) above 150 GeV around Cygnus X-1 corresponding to 78.9 minutes EOT between MJD 54002.928 and 54002.987 (2006-09-24). The black cross shows the best-fit position of the γ-ray source. The position of the X-ray source and radio emitting ring are marked by the green star and contour, respectively. The purple dots mark the directions tracked during the observations. Note that the bin contents are correlated due to the smoothing.

$0.6) \times 10^{-12}(E/1\text{ TeV})^{-3.2\pm0.6}\text{cm}^{-2}\text{s}^{-1}\text{TeV}^{-1}$ where the quoted errors are statistical only. We estimate the systematic uncertainty to be 35% on the overall flux normalization and 0.2 in the determination of the spectral index.

The excess from the direction of Cygnus X-1 occurred simultaneously with a hard X-ray flare detected by *INTEGRAL* [16], *Swift*/BAT and *RXTE*/ASM. Figure 4 shows the correlation between MAGIC, *Swift*/BAT and *RXTE*/ASM light-curves. The TeV excess was observed on the rising side of the first hard X-ray peak, 1–2 hours before its maximum, while there is no clear change in soft X-rays. Additionally, the MAGIC *non-detection* during the following night (yielding a 95% CL upper limit corresponding to a flux $\sim$5 times lower than the one observed in the second half of 2006-09-24) occurred during the decay of the second hard X-ray peak. A possible explanation is that, during the night of 2006-09-24, soft and hard X-rays were produced in different regions. Furthermore, hard X-rays and VHE γ-rays could be produced in regions linked by the colli-

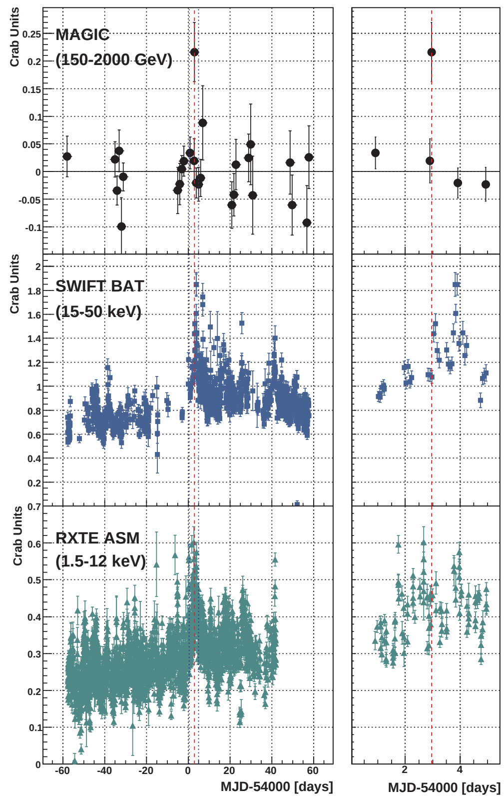

Figure 4: From top to bottom: MAGIC, *Swift*/BAT and *RXTE*/ASM measured fluxes from Cygnus X-1 as a function of time. The left panels show the whole time spanned by MAGIC observations. The vertical, dotted blue lines delimit the range zoomed in the right panels. The vertical red line marks the time of the MAGIC signal.

mated jet, e.g. the X-rays at the jet base and γ-rays at an interaction region between the jet and the stellar wind. These processes would have different physical timescales, thus producing a shift in time between the TeV and X-ray peaks. Note that the distance from the compact object to the TeV production region is constrained below $2'$ by MAGIC observations and therefore it is unrelated with the nearby radio emitting ring-like structure [8]. The observed TeV excess took place at phase 0.91 (phase 0.0 is when the BH is behind the O star). Currently, MAGIC observations at this phase value are available only for the night 2006-09-24, which precludes any possible analysis of periodicity for the TeV emission. The jet scenario, however, has some constraints. If the TeV emission were produced in the jet, well within the binary system, the photon-photon conversion in the stellar radiation field would be very substantial, rendering unlikely a TeV detection [17]. Admittedly, the inclination of the orbit and the angle of propagation to the observer can affect this. Even without an explanation for a TeV flare, it is possible that the emission could have originated far from the compact object. Interactions of the jet with the stellar wind may lead to such a situation.

In summary, for the first time we have found experimental evidence of VHE emission produced by a Galactic stellar-mass BH. It is also the first evidence of VHE gamma-rays produced at an accreting binary system. Our results show that a possible steady VHE flux is below the present IACT's sensitivity and tight upper limits have been derived. On the other hand, we find evidence for an intense flaring episode during the inferior conjunction of the optical star, on a timescale shorter than 1 day with a rise time of about 1 hour, correlated with a hard X-ray flare observed by *Swift* and *INTEGRAL*. These results imply the existence of a whole new phenomenology in the young field of VHE astrophysics of binary systems to be explored by present and future IACT's.

We thank the IAC for the excellent working conditions at the Observatorio del Roque de los Muchachos in La Palma.

References

[1] S. Bowyer, E. T. Byram, T. A. Chubb, H. Friedman, Cosmic X-ray Sources, Science 147 (1965) 394–398.

[2] J. Ziółkowski, Evolutionary constraints on the masses of the components of the HDE 226868/Cyg X-1 binary system, MNRAS 358 (2005) 851–859.

[3] D. R. Gies, C. T. Bolton, The optical spectrum of HDE 226868 = Cygnus X-1. II - Spectrophotometry and mass estimates, ApJ 304 (1986) 371–393.

[4] M. McConnell, et al., Gamma-Ray Variability of Cygnus X-1, APS Meeting Abstracts (2002) 17078–+.

[5] M. Cadolle Bel, et al., The broad-band spectrum of Cygnus X-1 measured by INTEGRAL, A&A 446 (2006) 591–602.

[6] A. M. Stirling, et al., A relativistic jet from Cygnus X-1 in the low/hard X-ray state, MNRAS 327 (2001) 1273–1278.

[7] G. E. Romero, M. M. Kaufman Bernadó, I. F. Mirabel, Recurrent microblazar activity in Cygnus X-1?, A&A 393 (2002) L61–L64.

[8] E. Gallo, R. Fender, C. Kaiser, D. Russell, R. Morganti, T. Oosterloo, S. Heinz, A dark jet dominates the power output of the stellar black hole Cygnus X-1, Nature 436 (2005) 819–821.

[9] F. Aharonian, et al., Discovery of the binary pulsar PSR B1259-63 in very-high-energy gamma rays around periastron with HESS, A&A 442 (2005) 1–10.

[10] J. Albert, et al., Variable Very-High-Energy Gamma-Ray Emission from the Microquasar LS I +61 303, Science 312 (2006) 1771–1773.

[11] F. Aharonian, et al., Discovery of Very High Energy Gamma Rays Associated with an X-ray Binary, Science 309 (2005) 746–749.

[12] V. Dhawan, M. Rupen, LS I +61 303 is a Be-Pulsar binary, not a Microquasar, in: VI Microquasar Workshop: Microquasars and Beyond, 2006.

[13] D. Khangulyan, F. Aharonian, V. Bosch-Ramon, On the formation of TeV radiation in LS 5039, ArXiv e-prints 707.

[14] A. Sierpowska-Bartosik, D. F. Torres, Pulsar model of the high energy phenomenology of LS 5039, ArXiv e-prints 708.

[15] J. Albert, et al., Very High Energy Gamma-Ray Radiation from the Stellar Mass Black Hole Binary Cygnus X-1, ApJ 665 (2007) L51–L54.

[16] M. Türler, et al., ATel 911 (2006) 1.

[17] W. Bednarek, F. Giovannelli, Very high energy gamma-ray production inside the massive binary system Cyg X-1/HDE 226868, A&A 464 (2007) 437–445.